PCCP

Accepted Manuscript

ROYAL SOCIETY OF CHEMISTRY

www.rsc.org/pccp

First-Principles Study on Hydrogen Evolution Reaction of VS_2 Nanoribbons

Yuanju Qu[1,2,3], Hui Pan[1]*, Chi Tat Kwok[2,1], and Zisheng Wang[3,1]

[1]Institute of Applied Physics and Materials Engineering, Faculty of Science and Technology, University of Macau, Macao SAR, P. R. China

[2] Department of Electromechanical Engineering, Faculty of Science and Technology, University of Macau, Macao SAR, P. R. China

[3] College of Physics and Communication Electronics, Jiangxi Normal University, Nanchang 330022, P. R. China

Abstract: Nanostructures have attracted increasing interests for applications in electrolysis of water as electrocatalysts. In this work, the edge-catalytic effects of one dimensional (1D) VS_2 nanoribbons with various edge configurations and widths have been investigated based on first-principle calculations. We show that the catalytic ability of VS_2 nanoribbon strongly depends on its edge structure, edge configuration, and width. We find that the S-edges of VS_2 nanoribbons are more active in electrolysis of water than V-edges due to their optimal free Gibbs energy for hydrogen evolution reaction in a wider range of hydrogen coverage. We also find that narrow nanoribbons show better catalytic performance than wide counterparts. We further show that the S-edge of narrow VS_2 nanoribbon with its V-edge covered by eight sulfur atoms has near-zero free Gibbs energy of hydrogen adsorption and comparable catalytic performance with Pt to an extent of hydrogen coverage, which is contributed to its metallic characteristic. We expect that VS_2 nanoribbons would be a promising 1D catalyst in electrolysis of water because of their impressive catalytic abilities both on the basal planes and edges.

Keywords: VS_2 nanoribbon, hydrogen production, hydrogen evolution reduction, first-principles calculations

* H. Pan (huipan@umac.mo); Tel: (853)88224427; Fax: (853)28838314

Introduction

Renewable green energy sources have been widely explored to replace traditional counterparts because of their limited natural resources and harmful side effects. As an ideal clean energy carrier, hydrogen is considered as one of the most important green candidates in renewable energy technologies. [1-3] Hydrogen can be produced by various methods. As a simple, clean, and promising way, electrolysis of water has been attracted increasing attention. [4] The efficiency for hydrogen production in the process is mainly determined by catalysts used. To date, noble metals, such as platinum, are the most stable and efficient catalysts. [5-7] However, the high cost and low abundance in nature limit their practical application. The realization of industrial hydrogen production requires efficient, stable and earth-abundant new materials to facilitate electrolyzing water into hydrogen. A lot of efforts have been carried out to find novel materials to replace platinum. [8-15] Recently, two-dimensional (2D) transition metal dichalcogenide monolayers, such as MoS_2, WS_2, and TiS_2, have been investigated as potential candidates to replace Pt due to their unique electronic, magnetic, and chemical properties. [16-37] It has been reported experimentally that MoS_2 nanoribbons showed good catalytic in electrolysis of water because of its active catalytic sites and high conductivity at edges. [25-27, 35] Based on density-functional-theory (DFT) calculations, Tsai et al. reported that the Mo-edge of MoS_2 shows better catalytic ability than its S-edge and found that doping can improve the hydrogen evolution reduction (HER) at its S-edge. [38-41] Most recently, Pan predicted that VS_2 monolayer shows high HER activity even at basal plane, which is

comparable with Pt at lower hydrogen coverage. [42] However, its catalytic performance strongly depended on the hydrogen coverage and was reduced at high hydrogen coverage due to reduced conductivity. Therefore, it's necessary to investigate the HER performance at the edges of VS_2 nanoribbons and find the mechanism to further improve its efficiency. In this work, we perform first-principles calculations to study the effects of edges on the HER activity of VS_2 nanoribbons with various edges structures and widths. We find that S-edges of VS_2 nanoribbons show active HER performance in electrolysis of water. We further show that narrow nanoribbons possess better catalytic abilities than wide ones.

Computational Method

We carry out the first-principles calculations to study the catalytic performance of the edges of VS_2 nanoribbons for applications in hydrogen production. The Vienna ab initio simulation package (VASP) [43] incorporated with projector augmented wave (PAW) scheme [44, 45], which is based on the density functional theory (DFT) [46] and the Perdew-Burke-Eznerhof generalized gradient approximation (PBE-GGA) [47], is used in our calculations. To avoid image-image interaction between two monolayers in neighbouring supercells, vacuum regions of at least 20 and 15 Å in vertical and parallel directions, respectively, were used. Based on Monkhorst and Pack scheme [43], a 1×1×1 grid for k-point sampling for geometry optimization of supercells, and 5×1×1 grid for the calculation of the density of states (DOS) are used.

An energy cut-off of 450 eV are consistently used in our calculations. Good convergence is obtained with these parameters and the total energy was converged to 2.0×10^{-5} eV/atom. Both spin-polarized and spin-unpolarized calculations are carried out to investigate the effect of magnetic moment on the catalytic capability.

Results and Discussion

In our calculations, VS_2 monolayer in rectangle configuration according to literature [23] is firstly constructed and optimized. Zigzag VS_2 nanoribbons are obtained by cutting the monolayer (Figure 1), because zigzag-edges are confirmed to be more stable and electrocatalytically active than armchair-edges in hydrogen adsorption. [16, 34] To investigate the effects of edges on the HER activity, two kinds of nanoribbons with different edge structures are constructed (Figures 1a&e), where one nanoribbon has four (half) sulfur atoms at its V-edge (called VS_2-NR-HS) (Figures 1a&b), and another one has eight (full) sulfur atoms at its V-edge (called VS_2-NR-FS) (Figures 1e&f). To investigate the effect of width on their HER performance, VS_2 nanoribbons with different widths are built up by taking one full honeycomb row off along the x-axis from the original nanoribbons at each time as indicated by the green dashed line and numbers (1, 2, 3, 4) (Figures 1a&e). The distances from its top V-edge to the dashed line marked with numbers are the widths of nanoribbons. The nanoribbons from the widest to the narrowest are named as VS_2-NR-HS(FS)-W (W = 1 - 4). The nanoribbons with various widths are fully relaxed to study the edge stability and their

HER performance. To investigate the effect of hydrogen coverage, the length of the nanoribbon is about 12.65 Å (4 unit cells along x-axis) (Figure 1).

The HER performance of VS_2 nanoribbon can be characterized by the free Gibbs reaction energy of hydrogen adsorption ΔG_H [38, 42, 48], which can be calculated from following equation:

$$\Delta G_H = \Delta E_H + \Delta E_{ZPE} - T\Delta S_H \qquad (1)$$

where ΔE_H is the hydrogen chemisorption energy defined as:

$$\Delta E_H = \mathrm{E(NR + nH)} - \mathrm{E(NR + (n-1)H)} - \frac{1}{2}E(H_2) \qquad (2)$$

and its average form is defined as:

$$\Delta E_H = \left[\mathrm{E(NR + nH)} - \mathrm{E(NR)} - \frac{n}{2}E(H_2)\right]/n \qquad (3)$$

where E(NR+nH) and E(NR) are total energies of VS_2 nanoribbons with and without hydrogen atoms at the edge, respectively. n is the number of H atoms adsorbed at the edges of VS_2 nanoribbons, and can be from 1 to 8 (for the edge with 8 sulfur atoms) (Figures 1d&g&h) or 1 to 4 (for the edge with 4 sulfur atoms) (Figure 1c) to investigate the effect of hydrogen coverage on catalytic activity. The hydrogen coverage refers to $\frac{n}{8}$ and $\frac{n}{4}$, respectively, for different edge structures. Therefore, ΔG_H as a function of the hydrogen coverage (n) can be obtained. $E(H_2)$ is the energy of hydrogen molecule, ΔS_H is the difference in entropy, and ΔE_{ZPE} is the difference in

zero point energy between the adsorbed and the gas phase. ΔE_{ZPE} - $T\Delta S_H$ is about 0.24 eV. So Eq. (1) is simplified to $\Delta G_H = \Delta E_H + 0.24$ [38, 48]. The reaction free energy of hydrogen adsorption calculated with Eq. (2) is referred to I-ΔG_H (individual process) and that calculated with Eq. (3) is referred to A-ΔG_H (average process).

We first study the V-edge of VS_2 nanoribbons with that covered by four sulfur atoms and various widths (VS_2-NR-HS-V-W) (W = 1 - 4) (Figures 1a&b). Various hydrogen coverages are realized by adding n hydrogen atoms onto the sulfur atoms at the edges (the orange dashed line in Figure 1c). We see that the calculated free Gibbs energies of VS_2-NR-HS-V-W in individual processes generally increase as hydrogen coverage increasing, and good HER activities may be achieved at certain hydrogen coverages, depending on the width of nanoribbons (Figure 2a). For example, the HER activities of wide nanoribbons (I-ΔG_H = -0.13 eV for VS_2-NR-HS-V-1, and I-ΔG_H = -0.09 eV for VS_2-NR-HS-V-2) are better than narrow ones (I-ΔG_H = -0.37 eV for VS_2-NR-HS-V-3 and I-ΔG_H = -0.33 eV for VS_2-NR-HS-V-4) at a hydrogen coverage of $\frac{2}{4}$ (Figure 2a). However, at hydrogen coverage of $\frac{3}{4}$, narrow nanoribbons (I-ΔG_H = -0.11 eV for VS_2-NR-HS-V-3, and I-ΔG_H = -0.13 eV for VS_2-NR-HS-V-4) show better HER activity than wider ones (I-ΔG_H = -0.24 eV for VS_2-NR-HS-V-1 and I-ΔG_H = 0.14 eV for VS_2-NR-HS-V-2). At full hydrogen coverage ($\frac{4}{4}$), VS_2-NR-HS-2 (ΔG_H = 0.14eV) shows the best catalytic performance in all of considered systems. The calculated A-ΔG_H as functions of hydrogen coverage in average processes show

the same trends as those in individual processes, but are negative. Although the A-ΔG_H of VS_2-NR-HS-V-2 is -0.14 eV at full hydrogen coverage, its catalytic performance should be not good because that the total reaction free energy needs to time the number of hydrogen atoms (four). Comparing the calculated reaction free energies in individual and average processes, we see that individual process is more likely to happen at high hydrogen concentration (from 50% to 100%). We also see that the V-edge of VS_2-NR-HS-4, shows better HER performance at 75% $\left(\frac{3}{4}\right)$ (A-ΔG_H = -0.31 eV) and 100% $(\frac{4}{4})$ (A-ΔG_H = -0.19 eV) than Mo-edge of MoS_2 nanoribbon at the same width (both above 0.6 eV at 75% and 100%) [38].

For the S-edges of VS_2 nanoribbons with V-edge covered by four sulfur atoms and various widths (VS_2-NR-HS-S-W, W = 1 - 4), the calculated free Gibbs energies for hydrogen adsorption in individual processes show oscillating phenomena as a function of hydrogen coverage (Figure 3a), which are in a range of 0.08 to 0.19 eV at even hydrogen coverages (n > 2), and 0.14 to 0.43 eV at odd hydrogen coverages (n > 2) (inset in Figure 3a). Among all of the four nanoribbons, the S-edge of the narrowest one (VS_2-NR-HS-4) shows the best HER performance, as indicated by the relatively low reaction free energies (ΔG_H = 0.08 eV, 0.13 eV, 0.16 eV) at a wide hydrogen coverage ($\frac{4}{8}$ to $\frac{6}{8}$ and $\frac{8}{8}$). The calculated ΔG_H in average processes show oscillating increment (from 0.08 eV to 0.2 eV) as hydrogen coverage increasing from $\frac{2}{8}$ to $\frac{8}{8}$ (Figure 3b). Similarly, the average process is more difficult to happen than

individual process if considering the number of hydrogen atoms when n > 2, but is easier at hydrogen coverage of $\frac{2}{8}$ because of low A-ΔG_H (0.08 eV) and high I-ΔG_H (-1.07 eV). Different from MoS_2 nanoribbons, where their S-edges are more catalytically inert comparing with Mo-edge [38, 39], the S-edge of VS_2 nanoribbons show interestingly better catalytic ability than their V-edges.

For another VS_2 nanoribbon with V-edge covered by eight sulfur atoms (Figures 1e&f), similarly, we firstly investigate the HER performance of V-edges of VS_2-NR-FS-V-W (W = 1 - 4). The relaxed structures of VS_2-NR-HS-V with various hydrogen coverages show that they are not stable at certain hydrogen coverages ($\frac{3}{8}$ and $\frac{4}{8}$) by broken V – S bonds, and forming hydrogen molecules. Therefore, their free adsorption energy ΔG_H's are not considered in these situations. The calculated A-ΔG_H show that only the V-edge of VS_2-NR-FS-4 is active at hydrogen coverages of $\frac{5}{8}$ and $\frac{7}{8}$ (0.11 eV and 0.12 eV, respectively) (S1).

In the case of S-edges of VS_2 nanoribbons with V-edge covered by eight sulfur atoms (VS_2-NR-FS-S-W, W = 1 - 4), the calculated ΔG_H show that excellent HER activities can be achieved (Figure 4). We see that the free Gibbs energies for hydrogen adsorption fluctuate around 0.2 eV with increasing hydrogen coverage, and the optimal catalytic performance of VS_2-NR-FS-S-1, 3 and 4 occur from $\frac{3}{8}$ to $\frac{8}{8}$ in the

individual processes (inset of Figure 4a). We also find that the catalytic performance of S-edges in VS_2-NR-FS is better than that in VS_2-NR-HS because of relatively low reaction free Gibbs energies (Figures 3a&4a). Interestingly, we see that the calculated A-ΔG_H of VS_2-NR-FS-S-1, 3, and 4 in average processes almost overlap with each other and increase from -0.12 to 0.1 eV as hydrogen coverage increases from $\frac{3}{8}$ to $\frac{8}{8}$ (Figure 4b). Particularly, the calculated A-ΔG_H of VS_2-NR-FS-S-1, 3, and 4 are near zero (0.013 eV, 0.006 eV, and 0.009 eV, respectively) at a hydrogen coverage of $\frac{5}{8}$, indicating high catalytic ability for average processes to happen. We see that the HER performance of S-edges of VS_2-NR-FS in average process is much better than that of VS_2-NR-HS (Figures 3b&4b). At the same time, the relaxed structures of VS2-NR-FS-3-W (W = 1-4) show that they are stable under various hydrogen coverages at their edges (S2&S3) and charge transfers from H atom to S atom (0.05 ~ 0.1 e). By comparing with literatures, we note that the activities of S-edges of VS_2-NR-FS (0.006 eV) are much higher than those of Mo-edges of MoS_2 (0.06 eV) and $MoSe_2$ (0.02 eV) nanoribbons, and W-edges of WS_2 (-0.04 eV) and WSe_2 (0.17 eV) nanoribbons under optimal performance conditions [39]. We further see that the HER performances of S-edges of VS_2-NR-FS is even better or comparable with the doped S-edges of MoS_2 nanoribbons [38]. The calculated free Gibbs energies in both individual and average processes show that the S-edges of VS_2-NR-FS are active in electrolysis of water at a wide hydrogen coverage (from $\frac{3}{8}$ to $\frac{8}{8}$) and show best performance at a moderate hydrogen coverage, which is comparable with Pt. We also carry out spin-polarized calculations and find that spin-alignment has negligible effect

on the calculated Gibbs free energy (S4). To reveal the origin of HER performance of S-edges in VS_2-NR-FS, the total densities of states (TDOSs) are calculated. The calculated TDOSs show that these nanoribbons are metallic, as indicated by the Fermi levels within conduction bands (Figures 5a-e). This high conductivity promises that S-edges of VS_2-NR-FS show high catalytic ability even at the vicinity of full hydrogen coverage.

To give a clear indication on the stability of VS_2 nanoribbon, it is necessary to study its formation possibility by calculating its edge energy (E_{edge}) as below:

$$E_{edge} = (E_{NR} - nE_{unit}(VS_2) - m\mu_S - l\mu_V)/2L \qquad (4)$$

where the edge energy has been normalized to the length of the edge. E_{NR} is the total energy of VS_2 nanoribbon, and E_{unit} (VS_2) is the energy of the VS_2 unit calculated from its monolayer. n is the total number of VS_2 units in the nanoribbon. μ_S and μ_V are the chemical potentials of one single atom calculated from bulk sulfur and vanadium, respectively. m and l are the numbers of extra S and V atoms at the edges of VS_2 nanoribbon, respectively. L is the nanoribbon's length. From the calculated edge energies of these two types of nanoribbons (Figure 6), we see that all the edge energies are slightly above zero and almost independent of width, indicating that these two types of nanoribbons can be achieved under suitable conditions. Importantly, the edge energies of VS_2 nanoribbons with V-edge covered by eight sulfur atoms

(VS_2-NR-FS) are lower than those with one edge covered by four sulfur atoms (VS_2-NR-HS) by 22 %, indicating the VS_2-NR-FS may be easier to be obtained in experiments. The easier formation of VS_2-NR-FS and its active edge in electrolysis of water indicate that they may find applications as catalysts in electrical hydrogen production.

Conclusion

We present a first-principles study on two types of zigzag VS_2 nanoribbons with various widths. We find that S-edges of VS_2 nanoribbons are more catalytically active than V-edges in electrolysis of water. Especially, the S-edges of VS_2 nanoribbons with V-edge covered by eight sulfur atoms show best HER catalytic performance in a wide range of hydrogen coverage and comparable activity with Pt at certain hydrogen coverages due to high conductivities. Our study further shows that narrow nanoribbons have overall better catalytic performances than wide counterparts. Our calculations demonstrate that the HER performance of 1D nanoribbon not only depends on edge atoms, but edge configurations and its width. It is expected that our findings may provide guidance on the design of electrocatalysts and find applications in electrolysis of water.

Acknowledgments

Hui Pan thanks the support of the Science and Technology Development Fund from Macau SAR (FDCT-068/2014/A2, FDCT-132/2014/A3, and FDCT-110/2014/SB) and Multi-Year Research Grants (MYRG2014-00159-FST and MYRG2015-00017-FST) and Start-up Research grant (SRG-2013-00033-FST) from Research & Development Office at University of Macau. The DFT calculations were performed at High Performance Computing Cluster (HPCC) of Information and Communication Technology Office (ICTO) at University of Macau.

Supporting information

Figures of the calculated free Gibbs energies of hydrogen adsorption on V-edges of VS_2-NR-FS-W (W = 1-4) in both individual and average processes. Relaxed structures and hydrogen chemisorption energies of VS_2-NR-FS-3-S with various hydrogen coverages from one to eight hydrogen atoms adsorbed. Spin polarization analysis of the S-edge of VS_2-NR-FS-3 as hydrogen coverage increases. The Supporting Information is available free of charge on the ACS Publications website.

References

[1] M. Wang, Z. Wang, X. Gong and Z. Guo, *Renew. Sust. Energy Rev.*, 2014, **29**, 573–588.

[2] B. Tamburic, P. Dechatiwongse, F. W. Zemichael, G. C. Maitland and K. Hellgardt, *Phys. Chem. Chem. Phys.*, 2013, **15**, 10783-10794.

[3] A. Datta, Physical Chemistry Chemical Physics, 2009, **11**, 11054–11059.

[4] K. Zeng and D. Zhang, *Prog. Energy Combust. Sci.*, 2010, **36**, 307–326.

[5] J. Greeley, T. F. Jaramillo, J. Bonde, I. Chorkendorff and J. K. Nørskov, *Nat. Mater.*, 2006, **5**, 909–913.

[6] J. H. Shim, Y. S. Kim, M. Kang, C. Lee and Y. Lee, *Phys. Chem. Chem. Phys.*, 2012, **14**, 3974-3979.

[7] M. E. Björketun, A. S. Bondarenko, B. L. Abrams, I. Chorkendorff and J. Rossmeisl, *Phys. Chem. Chem. Phys.*, 2010, **12**, 10536-10541.

[8] W. -F. Chen, K. Sasaki, Chao, A. I. Frenkel, N. Marinkovic, J. T. Muckerman, Y. Zhu and R. R. Adzic, *Angew. Chem. Int. Ed.*, 2012, **51**, 6131–6135.

[9] X. Chen, D. Wang, Z. Wang, P. Zhou, Z. Wu and F. Jiang, *Chem. Commun.*, 2014, **50**, 11683–11685.

[10] D. Wang, Z. Wang, C. Wang, P. Zhou, Z. Wu and Z. Liu, *Electrochem. Commun.*, 2013, **34**, 219–222.

[11] L. Feng, H. Vrubel, M. Bensimon and X. Hu, *Phys. Chem. Chem. Phys.*, 2014, **16**, 5917-5921.

[12] A. Lu, Y. Chen, H. Li, A. Dowd, M. B. Cortie, Q. Xie, H. Guo, Q. Qi and D.-L. Peng, *Int. J. Hydrog. Energy*, 2014, **39**, 18919–18928.

[13] M. D. Scanlon, X. Bian, H. Vrubel, V. Amstutz, K. Schenk, X. Hu, B. Liu and H. H. Girault, *Phys. Chem. Chem. Phys.*, 2013, **15**, 2847-2857.

[14] M. Chhowalla, H. S. Shin, G. Eda, L.-J. Li, K. P. Loh and H. Zhang, *Nat. Chem.*, 2013, **5**, 263–275.

[15] H. Pan, Y. P. Feng and J. Lin, *J. Comput. Theor. Nanos.*, 2010, **7**, 547–551.

[16] H. Pan and Y.-W. Zhang, *J. Mater. Chem.*, 2012, **22**, 7280-7290.

[17] J. N. Coleman, M. Lotya, A. O'Neill, S. D. Bergin, P. J. King, U. Khan, K. Young, A. Gaucher, S. De, R. J. Smith, I. V. Shvets, S. K. Arora, G. Stanton, H.-Y. Kim, K. Lee, G. T. Kim, G. S. Duesberg, T. Hallam, J. J. Boland, J. J. Wang, J. F. Donegan, J. C. Grunlan, G. Moriarty, A. Shmeliov, R. J. Nicholls, J. M. Perkins, E. M. Grieveson, K. Theuwissen, D. W. McComb, P. D. Nellist and V. Nicolosi, *Science*, 2011, **331**, 568–571.

[18] C. Lin, X. Zhu, J. Feng, C. Wu, S. Hu, J. Peng, Y. Guo, L. Peng, J. Zhao, J. Huang, J. Yang and Y. Xie, *J. Am. Chem. Soc.*, 2013, **135**, 5144–5151.

[19] D. Voiry, H. Yamaguchi, J. Li, R. Silva, D. C. B. Alves, T. Fujita, M. Chen, T.

Asefa, V. B. Shenoy, G. Eda and M. Chhowalla, *Nat. Mater.*, 2013, **12**, 850–855.

[20] Z. Wu, B. Fang, Z. Wang, C. Wang, Z. Liu, F. Liu, W. Wang, A. Alfantazi, D. Wang and D. P. Wilkinson, *ACS Catal.*, 2013, **3**, 2101–2107.

[21] H. Pan, *Sci. Rep.*, 2014, **4**, 7524.

[22] H. Pan and Y.-W. Zhang, *J. Phys. Chem. C*, 2012, **116**, 11752–11757.

[23] H. Pan, *J. Phys. Chem. C*, 2014, **118**, 13248–13253.

[24] Yandong, Y. Dai, M. Guo, C. Niu, J. Lu and B. Huang, *Phys. Chem. Chem. Phys.*, 2011, **13**, 15546-15553.

[25] J. Kibsgaard, Z. Chen, B. N. Reinecke and T. F. Jaramillo, *Nat. Mater.*, 2012, **11**, 963–969.

[26] M. V. Bollinger, J. V. Lauritsen, K. W. Jacobsen, J. K. Nørskov, S. Helveg and F. Besenbacher, *Phys. Rev. Lett.*, 2001, **87**, 196803.

[27] T. F. Jaramillo, K. P. Jorgensen, J. Bonde, J. H. Nielsen, S. Horch and I. Chorkendorff, *Science*, 2007, **317**, 100–102.

[28] Y. Yan, B. Xia, Z. Xu and X. Wang, *ACS Catal.*, 2014, **4**, 1693–1705.

[29] T.-Y. Chen, Y.-H. Chang, C.-L. Hsu, K.-H. Wei, C.-Y. Chiang and L.-J. Li, *Int. J. Hydrog. Energy*, 2013, **38**, 12302–12309.

[30] H. Wang, Z. Lu, S. Xu, D. Kong, J. J. Cha, G. Zheng, P.-C. Hsu, K. Yan,

D. Bradshaw, F. B. Prinz and Y. Cui, *Proc. Natl. Acad.Sci.*, 2013, **110**, 19701–19706.

[31] D. Merki and X. Hu, *Energy Environ. Sci.*, 2011, **4**, 3878-3888.

[32] Y. Li, H. Wang, L. Xie, Y. Liang, G. Hong and H. Dai, Journal of the American Chemical Society, 2011, **133**, 7296–7299.

[33] A. B. Laursen, S. Kegnæs, S. Dahl and I. Chorkendorff, *Energy Environ. Sci.*, 2012, **5**, 5577-5591.

[34] Y. Li, Z. Zhou, S. Zhang and Z. Chen, *J. Am. Chem. Soc.*, 2008, **130**, 16739–16744.

[35] H. Wang, C. Tsai, D. Kong, K. Chan, F. Abild-Pedersen, J. K. Nørskov and Y. Cui, *Nano Res.*, 2015, **8**, 566–575.

[36] Y. Ma, Y. Dai, M. Guo, C. Niu, Y. Zhu and B. Huang, ACS Nano, 2012, **6**, 1695–1701.

[37] H. Zhang, L.-M. Liu and W.-M. Lau, J. Mater. Chem. A, 2013, **1**, 10821-10828.

[38] C. Tsai, K. Chan, J. K. Nørskov and F. Abild-Pedersen, *Catal. Sci. Technol.*, 2015, **5**, 246–253.

[39] C. Tsai, K. Chan, F. Abild-Pedersen and J. K. Nørskov, *Phys. Chem. Chem. Phys.*, 2014, **16**, 13156-13164.

[40] C. Tsai, F. Abild-Pedersen and J. K. Nørskov, *Nano Lett.*, 2014, **14**, 1381–1387.

[41] C. Tsai, K. Chan, J. K. Nørskov and F. Abild-Pedersen, *Surf. Sci.*, 2015, **5**, 246-253.

[42] H. Pan, *Sci. Rep.*, 2014, 4, 5348.

[43] G. Kresse and J. Furthmüller, *Phys. Rev. B*, 1996, **54**, 11169–11186.

[44] J. P. Perdew, K. Burke and M. Ernzerhof, *Phys. Rev. Lett.*, 1996, **77**, 3865–3868.

[45] G. Kresse and D. Joubert, *Phys. Rev. B*, 1999, **59**, 1758–1775.

[46] P. Hohenberg and W. Kohn, *Phys. Rev.*, 1964, **136**, B864.

[47] P. E. Blöchl, *Phys. Rev. B*, 1994, **50**, 17953–17979.

[48] J. K. Nørskov, T. Bligaard, A. Logadottir, J. R. Kitchin, J. G. Chen, S. Pandelov and U. Stimming, *J. Electrochem. Soc.*, 2005, **152**, J23-J26.

Figure caption:

Figure 1, The representative structures of zigzag VS_2 nanoribbons with different edge structures and configurations: (a) top view of VS_2 nanoribbon with V-edge covered by four sulfur atoms (VS_2-NR-HS-W), (b) side view of VS2-NR-HS-W, (c) V-edge structure of VS_2-NR-HS-W, (d) S-edge structure of VS_2-NR-HS-W, (e) top view of VS_2 nanoribbon with V-edge covered by eight sulfur atoms (VS_2-NR-FS-W), (f) side view of VS2-NR-FS-W, (g) V-edge structure of VS_2-NR-FS-W, (h) S-edge structure of VS_2-NR-FS-W. Hydrogen atoms (white balls) are added to show their adsorption in Figures 1c, 1d, 1g&1h. The dashed orange line on hydrogen atoms indicates the way to remove hydrogen atoms one by one in Figure 1c&h. The width (W = 1 - 4) of VS_2 nanoribbon is the distance for the V-edge to the dashed green line and indicated it decreases.

Figure 2, Calculated overpotentials of V-edges of VS_2-NR-HS-W (W = 1 - 4) as a function of hydrogen coverage: (a) I-ΔG_H and (b) A-ΔG_H.

Figure 3, Calculated overpotentials of S-edges of VS_2-NR-HS-W (W = 1 - 4) as a function of hydrogen coverage: (a) I-ΔG_H and (b) A-ΔG_H.

Figure 4, Calculated overpotentials of S-edges of VS_2-NR-FS-W (W = 1 - 4) as a function of hydrogen coverage: (a) I-ΔG_H and (b) A-ΔG_H.

Figure 5, Calculated total density of states of VS_2-NR-FS-3 with a hydrogen coverage of: (a) 0, (b) 1/8, (c) 2/8, (d) 4/8 and (e) 8/8 at its S-edge.

Figure 6, Calculated edge energies of pure VS_2-NR-HS(FS)-W (W = 1 - 4).

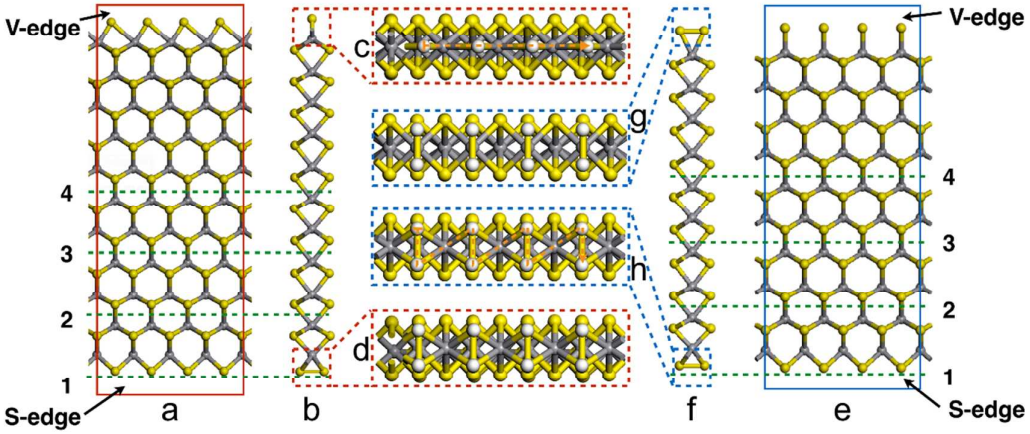

Figure 1

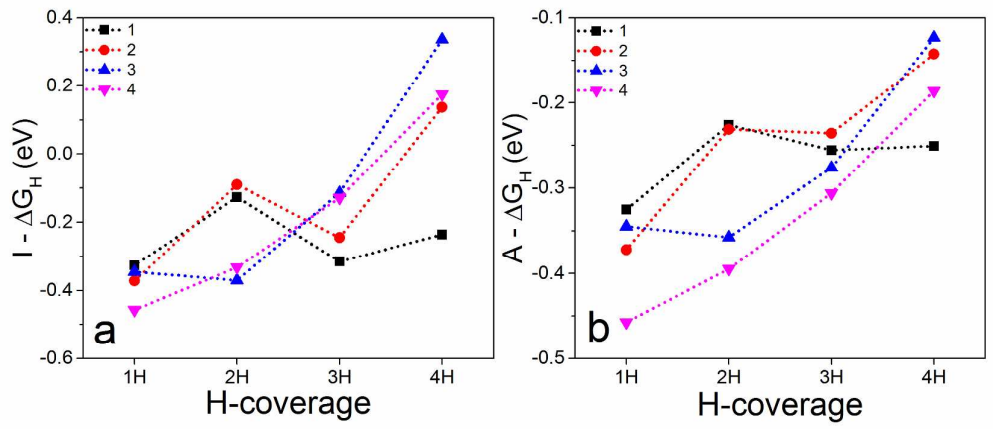

Figure 2

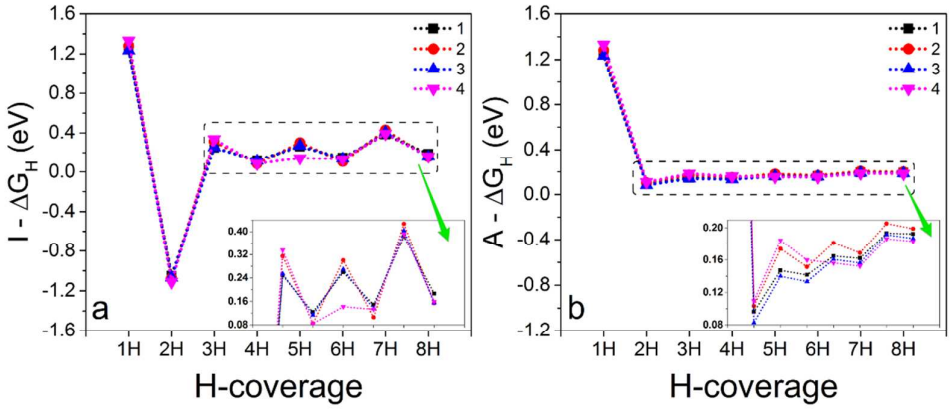

Figure 3

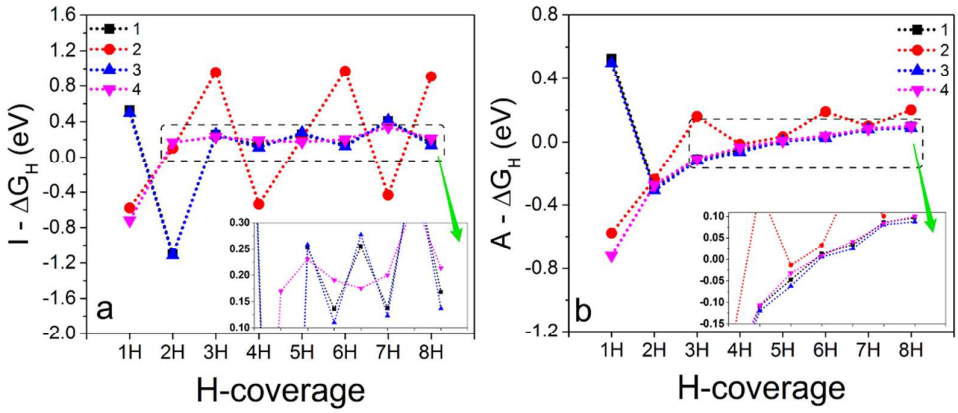

Figure 4

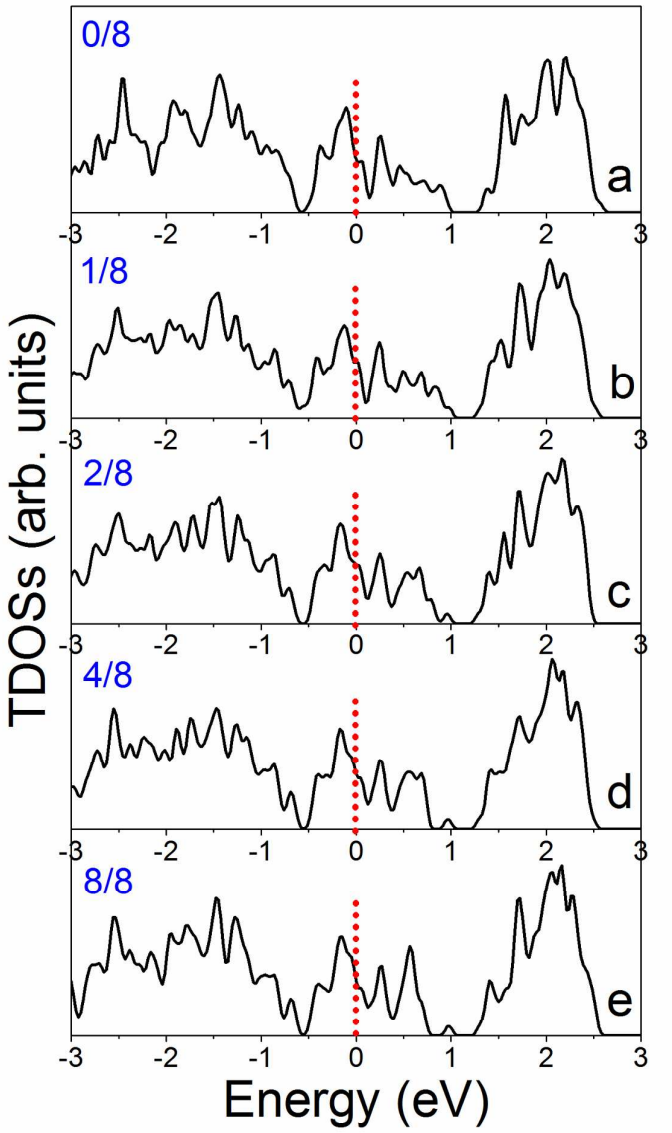

Figure 5

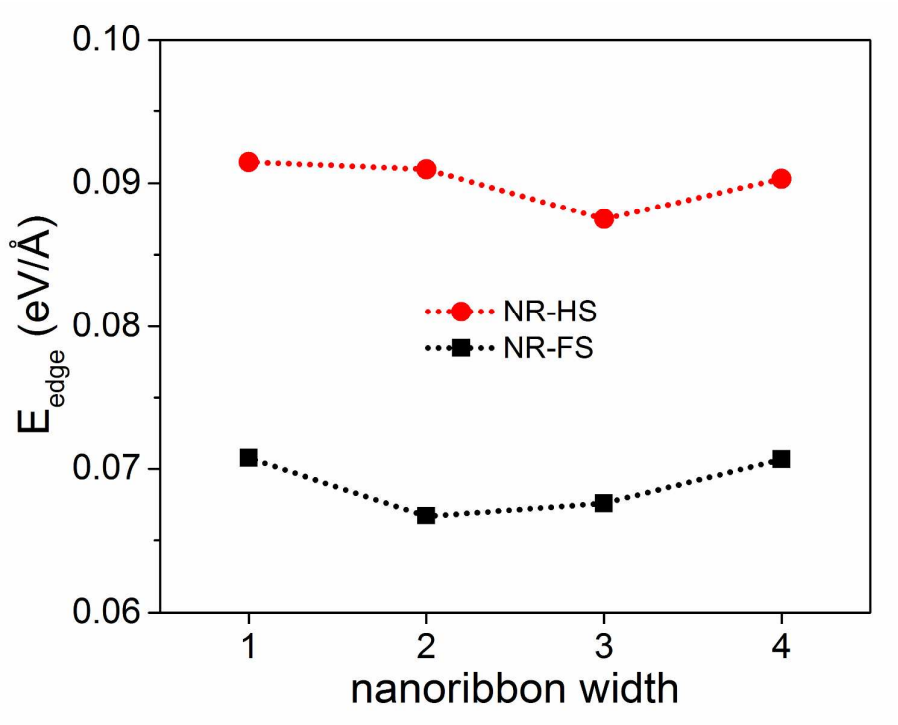

Figure 6

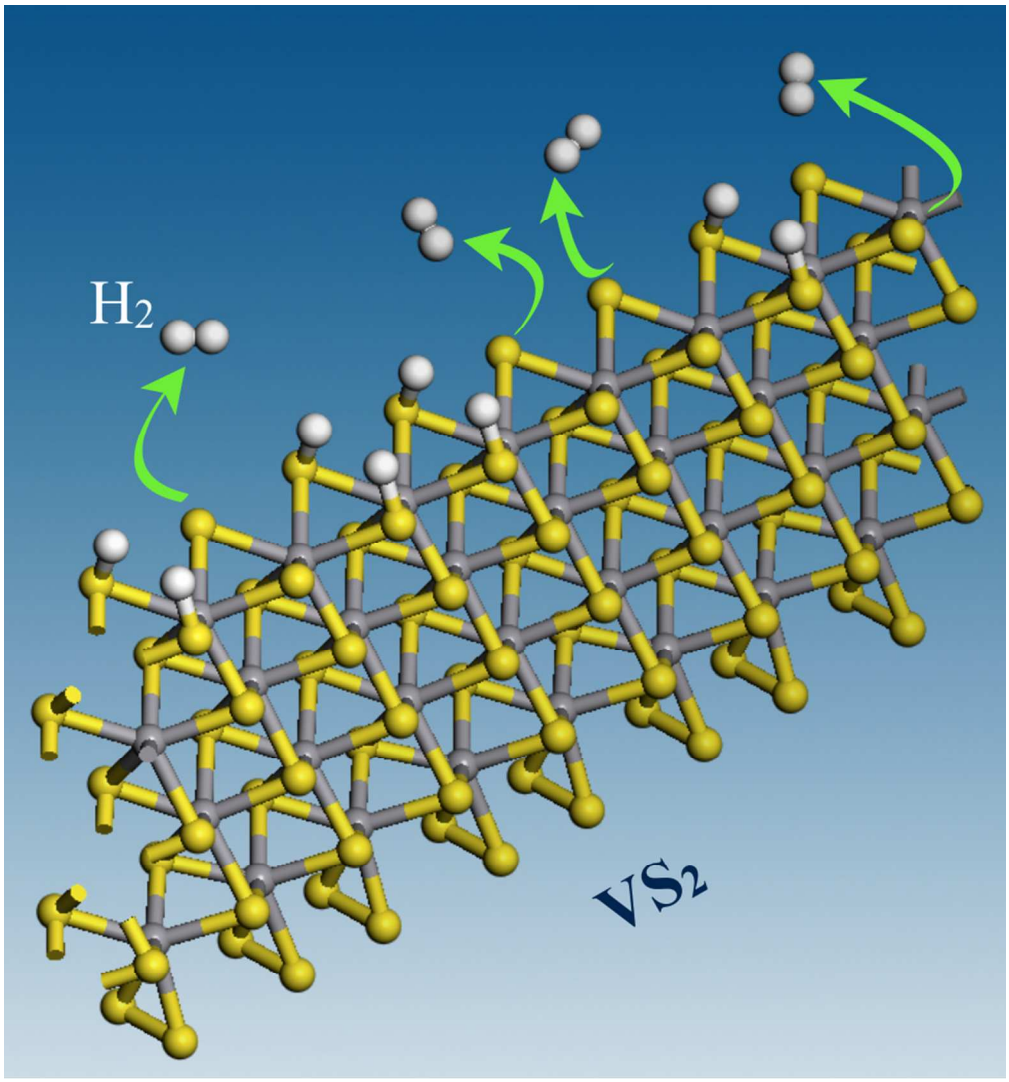

170x182mm (144 x 144 DPI)